Available online at www.sciencedirect.com
ScienceDirect
Trans. Nonferrous Met. Soc. China 26(2016) 1863−1870
Transactions of Nonferrous Metals Society of China
www.tnmsc.cn

Interaction among deformation, recrystallization and phase transformation of TA2 pure titanium during hot compression

Kai LI, Ping YANG

School of Materials Science and Engineering, University of Science and Technology Beijing, Beijing 100083, China

Received 14 July 2015; accepted 25 February 2016

Abstract: TA2 pure titanium was chosen to research the interaction among deformation, recrystallization and phase transformation during hot compression. The samples were hot compressed by thermal simulation method with different processing parameters. Variant selection induced by stress during cooling after compression was found. The prismatical texture component which featured that the [0001] direction perpendicular to the compressing direction produced preferentially under the compressing stress. As a result, the transformed α phase possesses strong prismatical texture which is different with the basal texture of compressed α phase. The minimum elastic strain energy is demonstrated to be the main reason that causes the variant selection. Dynamic recrystallization behavior and microstructure evolution during hot compression were also studied.

Key words: pure titanium; hot compression; phase transformation; texture; variant selection

1 Introduction

Hot deformation has much influence on the $\beta\rightarrow\alpha$ transformation and texture evolution which is found in many studies [1−3]. LIU et al [4] observed that compressing deformation can promote the $\beta\rightarrow\alpha$ transformation in TC4 titanium alloy when the alloy was compressed at 960 °C (5 °C under $\beta\rightarrow\alpha+\beta$ transus temperature). They also found that fine α phase grains could be obtained when the β grains were refined after compression. The deformation mechanism of hexagonal titanium alloys changes when they are deformed at different temperatures or with different processes. As a result, the textures in those alloys are always different. The texture aroused by cold rolling in pure titanium is a basal texture which deviates 15°−20° from the normal direction (ND) and the deviating angle decreases with the increasing strain [5]. Twinning usually occurs when the pure titanium is deformed at a low temperature [6,7]. Although the feature of texture in hot compressed titanium alloy has been studied early [8], its mechanism remains indistinct due to the complicated interaction between deformation and phase transformation.

Commercially pure titanium is usually deformed at the temperature around phase transus temperature [9]. The deforming mechanisms of the two phases in pure titanium would be much different. As a result, both the microstructure evolution and mechanical properties would be different between the two phases. Dynamic recrystallization is a significant way that could refine grains and enhance strength of titanium alloys. SU et al [10] compressed pure titanium at different temperatures with different strain rates to obtain the flow stress of commercially pure titanium under different compressing parameters. They found that dynamic recrystallization was a significant way to soften the pure titanium at high temperature.

The formation of texture in pure titanium is usually complicatedly influenced by both deformation and phase transformation. It is important to study the texture evolution during hot deformation in pure titanium. Inheritance during deformation and phase transformation has been reported [11−13]. LONARDELLI et al [11] compared the texture evolution between pure titanium and TC4 titanium alloy by means of cold rolling and heat treatment. They found that variant selection occurred more obviously in pure titanium and the strong texture is produced after cooling. GEY and HUMBERT [14] studied variant selection after cold rolling and annealing in a titanium alloy. Obvious variant selection was found during $\alpha\rightarrow\beta\rightarrow\alpha$ transformation after cold deformation and heat treatment which proved that deformation could induce preferred orientation. HUMBERT et al [15]

Corresponding author: Ping YANG; Tel: +86-10-82376968; E-mail: yangp@mater.ustb.edu.cn
DOI: 10.1016/S1003-6326(16)64302-9

considered that the strain energy hinders the precipitation of α phase and it is different at different grain boundaries. The reason for variant selection can be explained in terms of the theory of minimum elastic strain energy. Whereas, it is only applicative to the nucleation adjacent to grain boundary in this method, it remains indistinct why variant selections occur inside the grains after hot deformation.

Although hot deformation of commercially pure titanium has been studied, the feature of flow stress and dynamic recrystallization behavior during hot compression have not been researched fully. In addition, the influence of external stress on variant selection remains unclear during hot deformation. In this work, therefore, commercially pure titanium is compressed at high temperatures with different strain rates to investigate the influence of hot compression on phase transformation and variant selection.

2 Experimental

The forged TA2 commercially pure titanium was chosen to investigate the feature of phase transformation and variant selection in this work. Differential thermal analysis by 5 °C/min during heating and cooling was taken to obtain the $\beta\rightarrow\alpha$ phase transformation temperature. The result shows that an extremum occurred at the temperature of 897 °C, which indicates that the phase transformation temperature is 897 °C.

Cylindrical samples of 6 mm in diameter and 12 mm in height were manufactured from the original forged TA2 alloy. All the samples were heated to 920 °C and held for 20 min on a G1500−Gleeble simulating machine to get an entire β phase. Then, three samples were compressed at 920, 900 and 880 °C by 60% reduction with a strain rate of 0.01 s^{-1}. Another two samples were compressed at 920 °C with 1 and 5 s^{-1} to explore the influence on microstructure and texture of the material with different strain rates. To reveal the characterization of deformed α phase, another sample was held for 10 min at 880 °C and then compressed by 60% reduction with a strain rate of 0.01 s^{-1}. The samples were all water-quenched to room temperature after hot compression. Samples, cut perpendicularly to the compression plane, were electrolytically polished for electron backscatter diffraction (EBSD) test. EBSD system (Channel 5), mounted on an Ultra55 scanning electron microscope, was applied to revealing the orientation feature and texture evolution under compression.

3 Results

3.1 Stress−strain curves of different samples

True stress−strain curves are shown in Fig. 1. The stress is low when the samples are compressed at the β region which is shown with the dark curves. The true strength is enhanced with the increase of strain rate as the recovery of dislocations produced by compression would not be accomplished immediately. The blue curve of the sample held at 880 °C for 10 min shows a much higher strength than the samples compressed under β phase state. The α phase has a hexagonal structure which has less slip systems than BCC-β phase, so the deformation of α phase is more difficult than β phase.

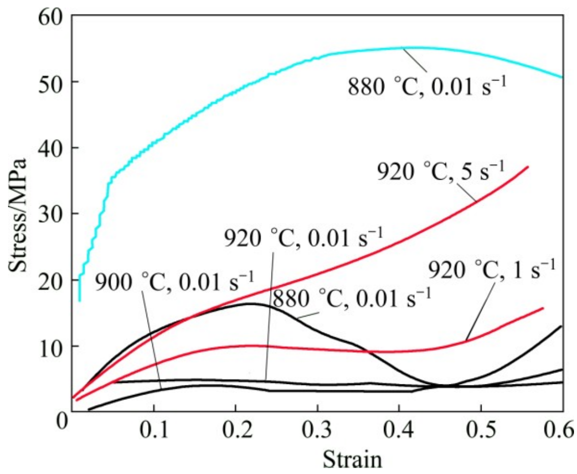

Fig. 1 True stress−strain curves of different samples

The sample compressed at 880 °C shows different properties with ones compressed at temperatures above transformation temperature. Stress decreases obviously after the strain reaching 0.2 due to two possible reasons. Either phase transformation or dynamic recrystallization may cause the decline of stress during hot deformation. As the microstructure of the ultimate α phase is mostly made up of deformed grains, it can be assumed that phase transformation is the main factor that leads to the decrease of stress.

The flow stress of the sample with only α phase increases quickly with the increase of strain at the beginning of compression. Then, the curve becomes flatter accompanying with the increase of strain, and the stress even decreases after the strain reaching 0.4. At the beginning of the compression, dislocation slipping is the main way for deformation. As the limitation of the number of slip systems in hexagonal titanium, dislocation slips more easily than in BCC titanium. Consequently, α phase presented an obviously higher strength than β phase. Dynamic recrystallization occurs obviously during compression under the drive of the increasing storage energy during deformation. And with the proportion of dynamic recrystallization increasing, the sample gets softened and the stress begins to fall down with the increasing strain.

3.2 Microstructure and microtexture of samples processed at different temperatures

The EBSD maps and relevant pole figures at different temperatures are shown in Figs. 2(a)−(c). Strong prismatical texture with {0001} plane parallel to the compressing direction (CD) and weak pyramidal texture component with {0001} plane angling 45° from the CD occur in the sample compressed at 920 °C. The prismatically-oriented grains in green and blue color are coarse and they are elongated in the compressing plane, whereas the pyramidally-oriented grains in purple color are fine and in irregular shape. The texture with $\langle 11\bar{2}0\rangle$ parallel to the CD occupies 61.3% and the percentage of the texture with $\langle 10\bar{1}0\rangle$ parallel to the CD is 10.1%. The samples compressed at 900 °C and 880 °C show generally similar texture containing strong prismatical texture and weak pyramidal texture, whereas Fig. 3 shows that the intensity of prismatical texture increases accompanying with the decline of compression temperature. It also reveals that the percentage of $\langle 10\bar{1}0\rangle$//CD component increases as the $\langle 11\bar{2}0\rangle$//CD component decreases within the prismatical texture. New α phase transformation would happen along with compression at 880 °C because the deformation temperature is lower than the transformation point. The new α-grains would approach to a stable orientation during the subsequent compression.

3.3 Microstructure and texture of samples processed with different strain rates

The pyramidally-oriented grains shown in Figs. 4(a) and (b) distribute dispersedly in the prismatically-oriented matrix with the strain rates of 1 s^{-1} and 5 s^{-1} which are different from the one compressed at 0.01 s^{-1}. Figure 5 shows that the grain size decreases with the increasing strain rate, which indicates that the raising of deformation rate could effectively refine α-grains. In addition, it also reveals that the decreasing deforming temperature could also do help for the reduction of grain size. With the increase of strain rate, the texture component of {0001} plane angling 35° from the CD occurs after transformation as shown in the yellow grains in Figs. 4(a) and (b). The formation of these grains with such new orientations may obey a different mechanism

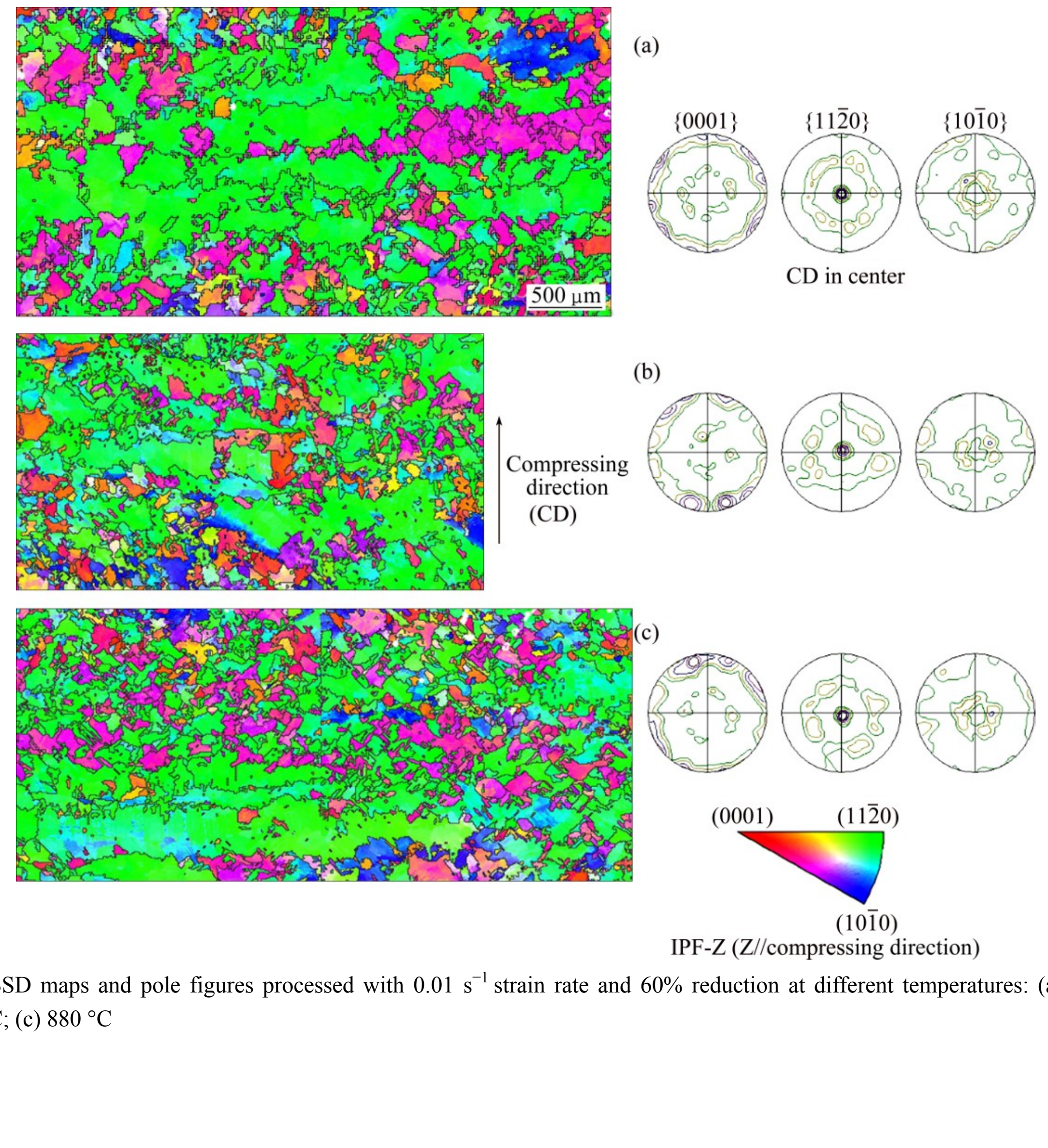

Fig. 2 EBSD maps and pole figures processed with 0.01 s^{-1} strain rate and 60% reduction at different temperatures: (a) 920 °C; (b) 900 °C; (c) 880 °C

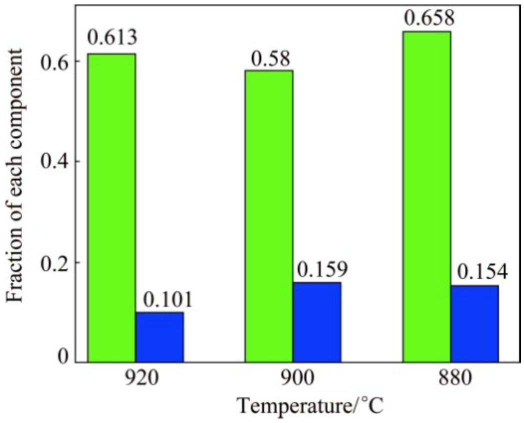

Fig. 3 Texture components of $\{11\bar{2}0\}$ in green and $\{10\bar{1}0\}$ in blue processed with 0.01 s^{-1} strain rate and 60% reduction at different temperatures

to prismatically-oriented grains and pyramidally-oriented grains.

3.4 Characterization of deformed *α* phase

To obtain entire *α* phase before compression, the sample was held for 10 min at 880 °C which is lower than the transformation temperature. Figure 6 shows the orientational feature of the compressed *α* phase. Basal texture is the main texture which has its {0001} parallel to the compressing plane. And it is obvious that the microstructure is heterogeneous after 60% compression. Some grains remained elongated, whereas many grains became refined and equiaxed during compression. This indicates that the dynamic recrystallization occurs in some grains.

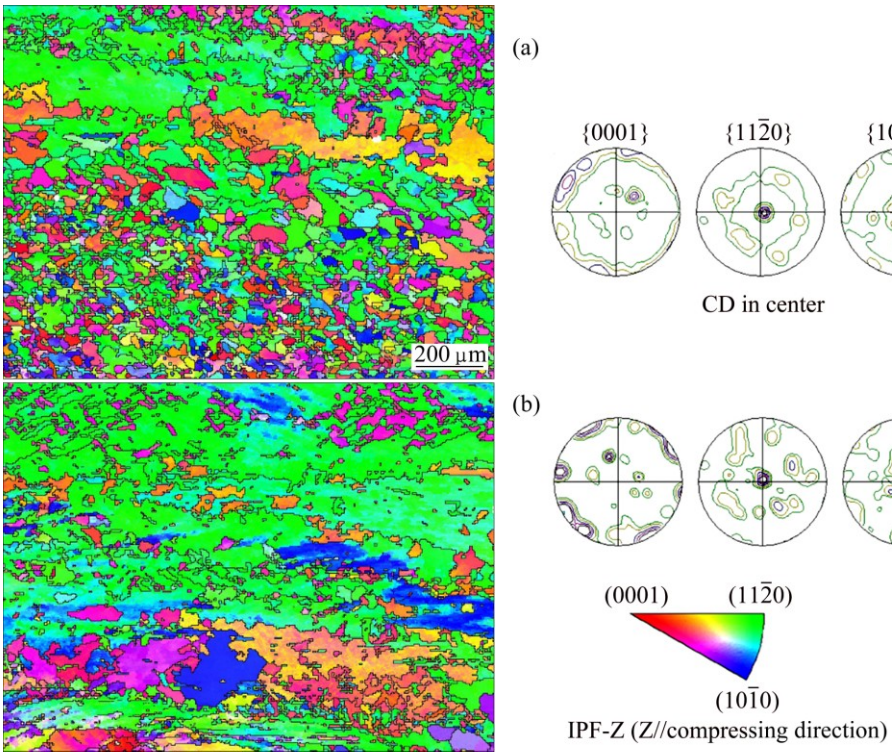

Fig. 4 EBSD maps and pole figures at 920 °C with 60% reduction under different strain rates: (a) 1 s^{-1}; (b) 5 s^{-1}

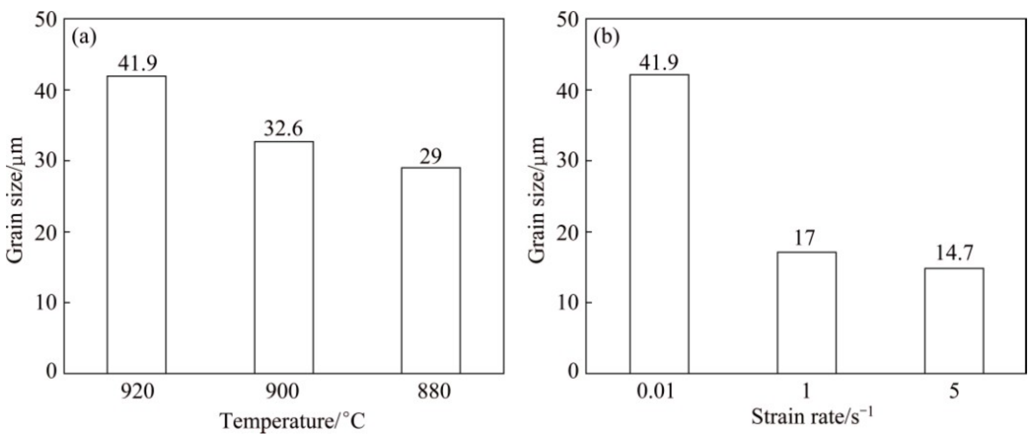

Fig. 5 Grain size distribution at different temperatures (a) and strain rates (b)

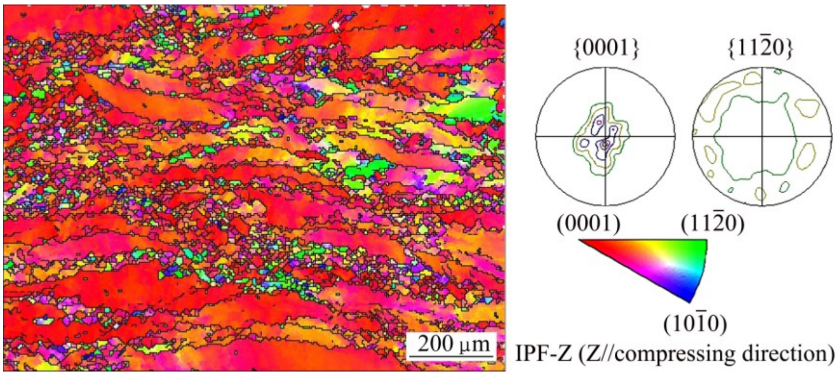

Fig. 6 EBSD map and pole figures of sample held at 920 °C for 20 min, then cooled to 880 °C and held for 10 min, compressed by 60% reduction with strain rate of 0.01 s^{-1}

4 Discussion

4.1 Microstructure and texture evolution

The β phase has a body-centered cubic (BCC) structure and the BCC metal usually develops ⟨001⟩ and ⟨111⟩ fiber texture during compression. Grains with ⟨001⟩ orientation can easily recover than other orientations. As a result, it is more compatible for the growth of ⟨001⟩ orientation grains under a low strain rate compression. Pure titanium mainly possesses strong ⟨001⟩ fiber texture mixed with weak ⟨111⟩ fiber after hot compression.

With the decrease of deforming temperature, phase transformation would happen earlier owing to the increase of transformation driving force. The increasing nucleation rate causes the reduction of grain size and dispersion of new α phase. More α grains have been deformed as they are more easily precipitated before the end of compression, which would enhance the intensity of {10$\bar{1}$0} texture component. More complex stress is aroused by the more variants during deformation, so the variant selection is partly weakened after phase transformation.

The intensity of texture gets weakened with the increasing strain rate. Additionally, a texture of {0001} angling 35° from the CD occurs at high strain rate. The texture of {111} may arise at a high deformation rate and the percentage of {111} texture increases along with the increase of strain rate according to our previous study on a near-β titanium alloy. The {111} β grains may produce the variant of 35°-tilting away from CD during phase transition according to Burgers orientation relationship which is shown in the yellow grains in Figs. 4(a) and (b). In conclusion, high strain rate can do help to decrease grain size and weaken the integral texture intensity.

4.2 Variant selection induced by stress

Many studies have indicated that a strong texture with {100} plane parallel to the compressing plane in β phase [16,17]. As a result, the main texture in this research might be a {100} texture as the samples are compressed almost in the single β phase region with 60% reduction. Moreover, the Burgers orientation relationship featured that $\{0001\}_\alpha//\{110\}_\beta$ and $\langle 11\bar{2}0\rangle_\alpha//\langle 111\rangle_\beta$, always occur between α and β phases. Therefore, it can be inferred from the orientation of generated α phase that the texture of β phase is indeed {100} component after hot compression. Two types of orientation would be obtained from the six {110} planes as the β phase has a feature of strong {100} texture. One characteristic orientation has its four {110} planes parallel to the CD and the other has a feature that two {110} planes angle 45° from the CD. As a result, the former one has two times intensity higher than the latter one. The {0001} plane of α phase should have a same characterization due to the Burgers orientation relationship, and the intensity of the pyramidal texture should be double to the prismatical texture without deformation. Whereas, it indicates that the intensity of the prismatical texture is much stronger than the pyramidal texture from the orientation maps in Fig. 2. It can be concluded that variant selection caused by compression distinctly occurs during $\beta\rightarrow\alpha$ transformation.

Figure 7(a) shows that the distance between the most close-packed planes is increased with a strain of ε_3 during $\beta\rightarrow\alpha$ transformation as the interplanar spacing of $\{110\}_\beta$ is 0.228 nm and the interplanar spacing of $\{0001\}_\alpha$ is 0.234 nm. Therefore, compressing stress would restrain the transformation which has its {110} crystal plane perpendicular to the CD and promote the one parallel to the CD. As a result, the prismatically-oriented variant could preferentially form and the pyramidally-oriented variant is restrained.

Locations of atoms would be adjusted in the close-packed planes during transformation as shown in Fig. 7(b). The atoms in {110} plane contract with ε_1 along [1$\bar{1}$0] direction and by expending with ε_2 along the [001] direction. Variant might be generated

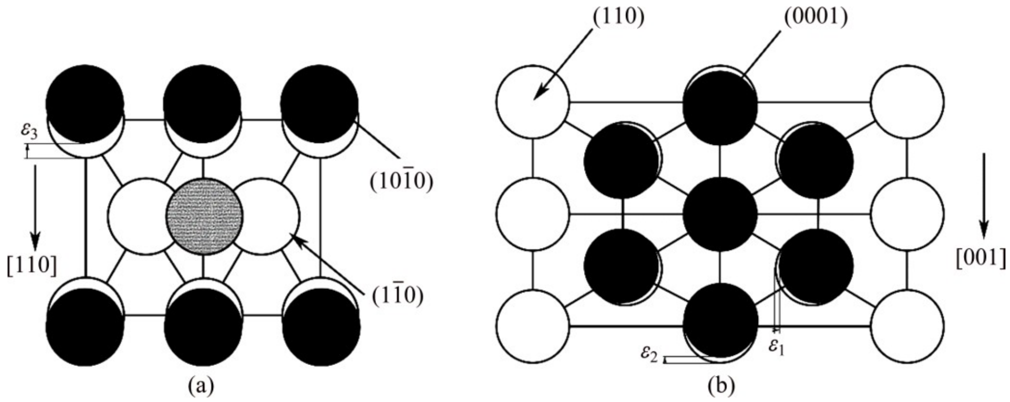

Fig. 7 Atom distortion during phase transformation in $(1\bar{1}0)_\beta/(10\bar{1}0)_\alpha$ (a) and $(110)_\beta/(0001)_\alpha$(b) (BCC atoms in white and HCP structure in black)

preferentially if compressing stress is exerted along a [001] direction in {110} plane. The prismatically-oriented variant in this work exactly meets the condition above, as a result, the prismatically-oriented variant selection occurs and the intensity of prismatical texture is strengthened.

The elastic strain energy increases to hinder the phase transformation as the lattice distortion during the generation of the new α phase. The value of the elastic strain energy could be expressed by

$$E=-1/2\sigma^{\mathrm{I}}\varepsilon^{\mathrm{tr}} \tag{1}$$

where $\varepsilon^{\mathrm{tr}}$ represents the transformation strain which is a constant value as the lattice distortion is fixed; σ^{I} is the stress caused by both phase transformation and deformation. An equation is proposed to calculate the influence by these two factors:

$$\sigma^{\mathrm{I}}=\sigma^{\mathrm{tr}}+\sigma^{\mathrm{ex}} \tag{2}$$

$$E=-1/2\sigma^{\mathrm{tr}}\varepsilon^{\mathrm{tr}}-1/2\sigma^{\mathrm{ex}}\varepsilon^{\mathrm{tr}} \tag{3}$$

where σ^{tr} represents the stress induced by transformation strain and σ^{ex} represents the stress within the samples caused by external force during hot compression. σ^{ex} can be expressed by

$$\sigma^{\mathrm{ex}}=\begin{bmatrix}0&0&0\\0&0&0\\0&0&\sigma\end{bmatrix} \tag{4}$$

And the transformation strain of both prismatically-oriented grain and pyramidally-oriented grain can be expressed by the following matrixes:

$$\varepsilon_{\mathrm{pr}}^{\mathrm{tr}}=\begin{bmatrix}\varepsilon_x&0&0\\0&\varepsilon_y&0\\0&0&\varepsilon_2\end{bmatrix} \tag{5}$$

$$\varepsilon_{\mathrm{py}}^{\mathrm{tr}}=\begin{bmatrix}\varepsilon_x&0&0\\0&\varepsilon_y&0\\0&0&-0.707\varepsilon_3+0.707\varepsilon_2\end{bmatrix} \tag{6}$$

It can be easily deduced that $E_{\mathrm{pr}}<E_{\mathrm{py}}$ which means that less elastic strain energy is needed to be overcome for the generation of prismatically-oriented variant, therefore, the compressing stress can lead to variant selection which promotes the formation of prismatical texture.

4.3 Interaction among deformation, phase transformation and recrystallization

It's quite different between the prismatically-oriented grains and pyramidally-oriented grains. The β phase grains are elongated perpendicular to the CD during compression. The elongated shape of β is remained after phase transformation so that the prismatically-oriented grains have a similar morphology. However, the pyramidally-oriented grains disperse equiaxially among the prismatically-oriented matrix. It is distinctly inferred that the pyramidally-oriented grains are produced during cooling after the formation of elongated grains.

Misorientations in different grains are shown in Figs. 8(d)−(f). Pyramidally-oriented grains with purple color present low misorientation while large misorientation is found in a single prismatically-oriented grain. Deformation in each β grain is heterogeneous during hot compression and some grains have relatively large misorientations. It can be seen that most of β grains transform into a single α grain. As a result, large misorientation of parent grain may be inherited by product grains during compression as the phase transformation obeys the Burgers orientation relationship strictly. The orientations of some prismatically-oriented grains rotate from $\langle 11\bar{2}0\rangle$ to $\langle 10\bar{1}0\rangle$. It can be

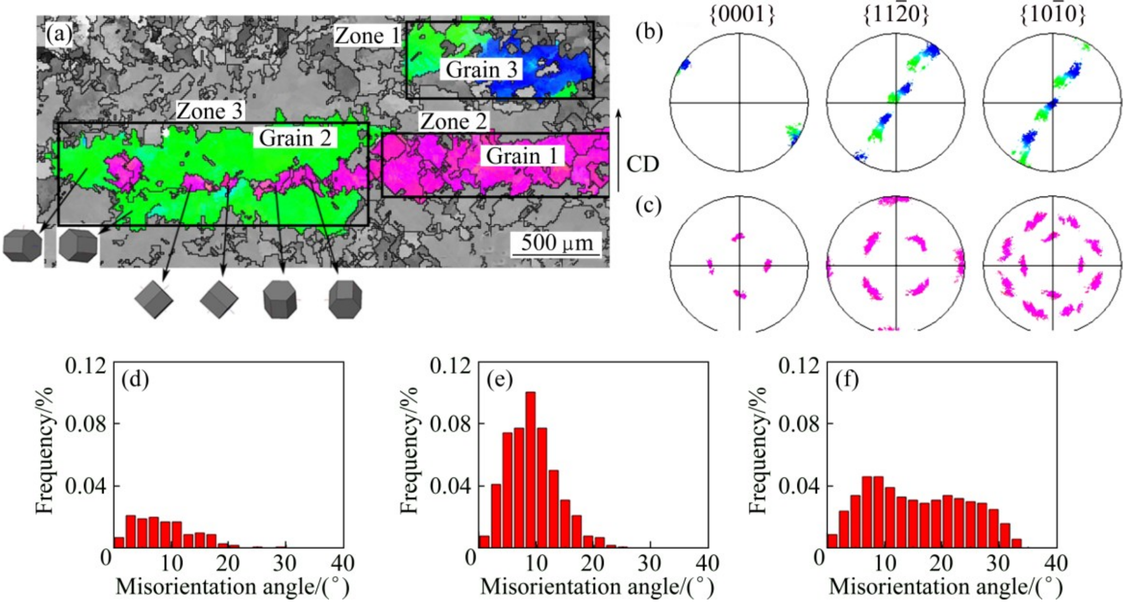

Fig. 8 Orientational characterizations of some special grains at 920 °C, 0.01 s^{-1} compression: (a) IPF maps; (b, c) Pole figures related to Zones 1 and 2, respectively; (d−f) Misorientations related to Grains 1−3, respectively

inferred that some deformed β grains have orientations rotating from ⟨001⟩ to ⟨112⟩ paralleling to compression direction, whereas the pyramidally-oriented grains are almost equiaxial which have different morphologies with the deformed grains. It can be concluded from the equiaxial shape of pyramidally-oriented grains that β grains are partially recrystallized.

The deformed β phase is more appropriate for the precipitation of α phase than the recrystallized β phase because of its high storage energy caused by deformation. As a result, the prismatically-oriented grains form earlier than the pyramidally-oriented grains. The external stress will be released by the former prismatically-oriented grains which have a reversed strain with the external stress during transformation. Meanwhile, the generation of the former variant induces a local strain caused by phase transition. Pyramidally-oriented variant precipitates to release the strain caused by the former variant. Zone 3 in Fig. 8(a) shows that fine pyramidally-oriented variant generates between two large prismatically-oriented grains. The two perpendicular prismatically-oriented grains are formed ahead while some recrystallized β phases are remained. Subsequently, four other variants occur preferentially under the stress produced by the two prismatically-oriented grains.

5 Conclusions

1) Compressed α phase possesses a basal texture which has its {0001} plane perpendicular to compressing direction. With the influence of interaction of deformation and phase transformation, the transformed α phase possesses strong prismatical texture with weak pyramidal texture which is inherited from the compressed β phase with strong {001} texture.

2) Obvious variant selection occurs during phase transformation under hot compression since the elastic strain energy is minimum in prismatically-oriented grains.

3) Dynamic recrystallization can easily happen in α phase than in β phase as its higher stored energy after compression and the β phase retains highly recovery state with deformed morphology after compression. Deformation in α phase-region contributes to refining grains in pure titanium.

References

[1] ZENG Z, JONSSON S, ROVEN H J. The effects of deformation conditions on microstructure and texture of commercially pure Ti [J]. Acta Materialia, 2009, 57: 5822−5833.

[2] GERMAIN L, GEY N, HUMBERT M, VO P, JAHAZI M, BOCHER P. Texture heterogeneities induced by subtransus processing of near α titanium alloys [J]. Acta Materialia, 2008, 56: 4298−4308.

[3] QIN Chun, YAO Ze-kun, NING Yong-quan, SHI Zhi-feng, GUO Hong-zhen. Hot deformation behavior of TC11/Ti−22Al−25Nb dual-alloy in isothermal compression [J]. Transactions of Nonferrous Metals Society of China, 2015, 25(7): 2195−2205.

[4] LIU B, LI Y, MATSUMOTO H, KOIZUMI Y, LIU Y, CHIBA A. Enhanced grain refinement through deformation induced α precipitation in hot working of α+β titanium alloy [J]. Advanced Engineering Materials, 2012, 14: 785−789.

[5] MILNER J L, ABU-FARHA F, KURFESS T, HAMMOND V H. Effects of induced shear deformation on microstructure and texture evolution in CP-Ti rolled sheets [J]. Materials Science and Engineering A, 2014, 619: 12−25.

[6] QIN H, JONAS J J. Variant selection during secondary and tertiary twinning in pure titanium [J]. Acta Materialia, 2014, 75: 198−211.

[7] ZENG Z, ZHANG Y, JONSSON S. Microstructure and texture evolution of commercial pure titanium deformed at elevated temperatures [J]. Materials Science and Engineering A, 2009, 513−514: 83−90.

[8] MOUSTAHFID H, HUMBERT M, PHILIPPE M J. Modeling of the texture transformation in a Ti-64 sheet after hot compression [J]. Acta Materialia, 1997, 45: 3785−3790.

[9] XU Chun, ZHU Wen-feng. Transformation mechanism and mechanical properties of commercially pure titanium [J]. Transactions of Nonferrous Metals Society of China, 2010, 20(11): 2162−2167.

[10] SU J H, HAN Y W, REN F Z, CHEN Z Q. Dynamic recrystallization behavior of pure titanium [J]. Advanced Materials Research, 2014, 852: 66−70.

[11] LONARDELLI I, GEY N, WENK H R, HUMBERT M, VOGEL S C, LUTTEROTTI L. In situ observation of texture evolution during $\alpha\rightarrow\beta$ and $\beta\rightarrow\alpha$ phase transformations in titanium alloys investigated by neutron diffraction [J]. Acta Materialia, 2007, 55: 5718−5727.

[12] DAYMOND M R, HOLT R A, CAI S, MOSBRUCKER P, VOGEL S C. Texture inheritance and variant selection through an hcp–bcc–hcp phase transformation [J]. Acta Materialia, 2010, 58: 4053−4066.

[13] SHI R, DIXIT V, FRASER H L, WANG Y. Variant selection of grain boundary a by special prior β grain boundaries in titanium alloys [J]. Acta Materialia, 2014, 75: 156−166.

[14] GEY N, HUMBERT M. Characterization of the variant selection occurring during the alpha→beta→alpha phase transformations of a cold rolled titanium sheet [J]. Acta Materialia, 2002, 50: 277−287.

[15] HUMBERT M, GERMAIN L, GEY N, BOCHER P, JAHAZI M. Study of the variant selection in sharp textured regions of bimodal IMI 834 billet [J]. Materials Science and Engineering A, 2006, 430: 157−164.

[16] LI L, LUO J, YAN JJ, LI MQ. Dynamic globularization and restoration mechanism of Ti−5Al−2Sn−2Zr−4Mo−4Cr alloy during isothermal compression [J]. Journal of Alloys and Compounds, 2015, 622: 174−183.

[17] FAN J K, KOU H C, LAI M J, TANG B, CHANG H, LI J S. Hot deformation mechanism and microstructure evolution of a new near β titanium alloy [J]. Materials Science and Engineering A, 2013, 584: 121−132.

TA2 纯钛在热压缩过程中形变、再结晶与相变的交互作用

李 凯，杨 平

北京科技大学 材料科学与工程学院，北京 100083

摘 要：选取 TA2 合金进行压缩来研究纯钛在热压缩过程中形变、再结晶与相变的交互作用规律，在不同的变形参数下进行热模拟压缩实验。实验发现，在热压缩之后的冷却过程中有明显的变体选择现象发生，在压应力作用下[0001]垂直于压缩方向的柱面织构组分会优先形成，因此会造成通过相变而产生的强柱面织构与变形 α 相所产生的强基面织构有明显的不同。研究表明，形成最小的弹性应变能是促使变体选择产生的主要原因。同时，对 TA2 纯钛在热变形过程中的再结晶规律和组织转变特征进行了研究。

关键词：纯钛；热压缩；相变；织构；变体选择

(Edited by Xiang-qun LI)